

Development of Novel, Highly Potent Inhibitors of V-RAF Murine Sarcoma Viral Oncogene Homologue B1 (BRAF): Increasing Cellular Potency through Optimization of a Distal Heteroaromatic Group

Bart M. J. M. Suijkerbuijk,^{†,§} Ion Niculescu-Duvaz,^{†,§} Catherine Gaulon,[†] Harmen P. Dijkstra,[†] Dan Niculescu-Duvaz,[†] Delphine Ménard,[†] Alfonso Zambon,[†] Arnaud Nourry,[†] Lawrence Davies,[†] Helen A. Manne,[†] Frank Friedlos,[†] Lesley M. Ogilvie,[†] Douglas Hedley,[†] Filipa Lopes,[†] Natasha P. U. Preece,[†] Javier Moreno-Farre,[†] Florence I. Raynaud,[†] Ruth Kirk,[‡] Steven Whittaker,[‡] Richard Marais,[‡] and Caroline J. Springer^{*,†}

[†]The Institute of Cancer Research, Cancer Research UK Centre for Cancer Therapeutics, 15 Cotswold Road, Sutton, Surrey SM2 5NG, United Kingdom, and [‡]The Institute of Cancer Research, Cancer Research UK Centre for Cell and Molecular Biology, 237 Fulham Road, London SW3 6JB, United Kingdom. [§]These authors contributed equally to this work.

Received May 8, 2009

We describe the design, synthesis, and optimization of a series of new inhibitors of V-RAF murine sarcoma viral oncogene homologue B1 (BRAF), a kinase whose mutant form (V600E) is implicated in several types of cancer, with a particularly high frequency in melanoma. Our previously described inhibitors with a tripartite A–B–C system (where A is a hinge binding pyrido[4,5-*b*]imidazolone system, B is an aryl spacer group, and C is a heteroaromatic group) were potent against purified V600E BRAF *in vitro* but were less potent in accompanying cellular assays. Substitution of different aromatic heterocycles for the phenyl based C-ring is evaluated herein as a potential means of improving the cellular potencies of these inhibitors. Substituted pyrazoles, particularly 3-*tert*-butyl-1-aryl-1*H*-pyrazoles, increase the cellular potencies without detrimental effects on the potency on isolated V600E BRAF. Thus, compounds have been synthesized that inhibit, with low nanomolar concentrations, V600E BRAF, its downstream signaling in cells [as measured by the reduction of the phosphorylation of extracellular regulated kinase (ERK)], and the proliferation of mutant BRAF-dependent cells. Concomitant benefits are good oral bioavailability and high plasma concentrations *in vivo*.

Introduction

V-RAF murine sarcoma viral oncogene homologue B1 (BRAF^{v600E}) is a serine/threonine kinase that operates downstream from RAS and is responsible for activation of MAPK/ERK kinase (MEK) and extracellular regulated kinase (ERK) activation in the mitogen-activated protein kinase (MAPK) pathway, a conserved signaling cascade responsible for cell proliferation and survival.^{1,2} Recent studies have shown that mutations in *BRAF* are found in a number of cancers, such as melanomas, ovarian, colorectal, and papillary thyroid cancers.³ Melanomas in particular show a high incidence of *BRAF* mutations, the most common being a substitution of glutamic acid for valine at position 600 (V600E).⁴ This point mutation lies within the activation segment of the protein, adjacent to the conserved DFG motif, and stimulates constitutive kinase activity in BRAF.⁵ This, in turn, causes continuous activation of MEK and ERK, the latter of which phosphorylates several cytosolic enzymes and nuclear substrates.

ERK controls gene expression, cytoskeletal rearrangements, and metabolism, causing cell transformation and contributing to tumor initiation and maintenance. Targeting this pathway, for example, through inhibition of BRAF, is therefore a main focus point of many current cancer therapeutics approaches.^{6–12}

X-ray crystallographic studies of the kinase domain of protein kinases together with structural probing by classical medicinal chemistry have been important for the development of specifically designed small molecule inhibitors that bind to specific protein kinases with high association constants. The application of these techniques in the development of new anticancer drugs has led to the discovery of a number of highly successful kinase inhibitors, such as sorafenib,^{13,14} gefitinib,¹⁵ and imatinib,^{16–18} as well as erlotinib,¹⁹ sunitinib,²⁰ and dasatinib²¹ (see Figure 1).

Given the importance of BRAF as a therapeutic target,^{9,22} we initiated a program to develop a series of small molecule BRAF inhibitors.^{23–27} The design and synthesis of novel BRAF inhibitors based on a 7-substituted 1*H*-imidazo[4,5-*b*]pyridin-2(3*H*)-one hinge binding fragment (ring A in Figure 2) connected to a substituted 1,4-phenylene or a 1,4-naphthalene fragment (ring B in Figure 2) that in turn is attached to a substituted aromatic group (ring C in Figure 2) via a urea linker have been described.²⁵ In addition, we have shown that the overall potencies of these inhibitors could be greatly enhanced by appropriate B-ring functionalization.²⁶

*To whom correspondence should be addressed. Phone: +44 20 87224214. Fax: +44 20 8722 4046. E-mail: caroline.springer@icr.ac.uk.

^aAbbreviations: RAF, rapidly growing fibrosarcoma; BRAF, V-RAF murine sarcoma viral oncogene homologue B1; MAPK, mitogen-activated protein kinase; MEK, mitogen-activated protein kinase/extracellular regulated kinase; ERK, extracellular regulated kinase; SRB, sulforhodamine B; PK, pharmacokinetics; THF, tetrahydrofuran; DMSO, dimethyl sulfoxide; SAR, structure–activity relationship; *F*, percent oral bioavailability.

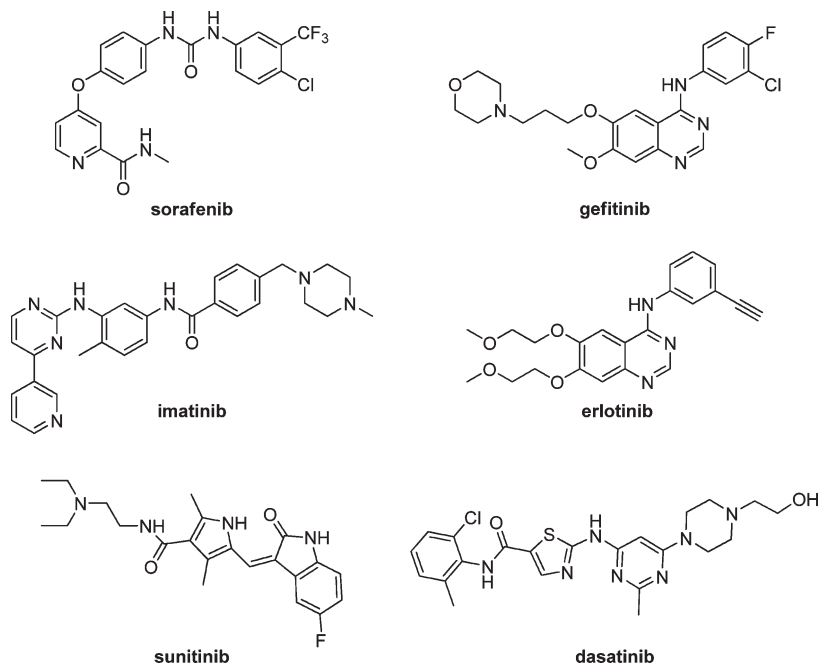


Figure 1. Structural formulas of recently developed kinase inhibitors.

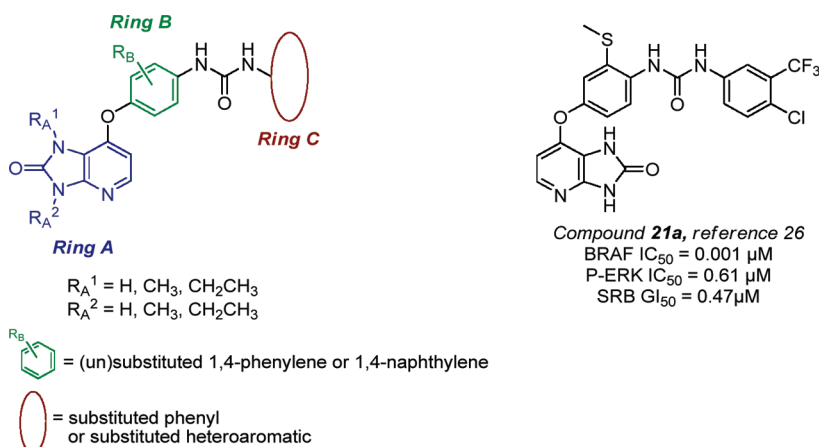


Figure 2. General structural formulas of the BRAF inhibitors and one representative example.

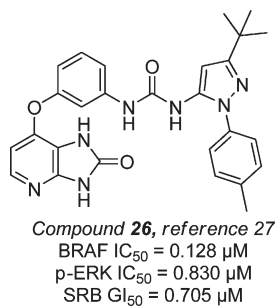


Figure 3. Structural formula of 1,3-phenylene compound with pyrazole ring C and biological data.

The inhibitors thus obtained exhibit BRAF IC_{50} values as low as 1 nM, but their potencies on cells (pERK IC_{50} and sulforhodamine B (SRB) GI_{50} on BRAF-dependent cells) are on the order of several hundred nanomolar (for example, compound 21a from ref 26; Figure 2).

On the basis of docking studies, we developed a new series of BRAF inhibitors with the same tripartite structure (rings

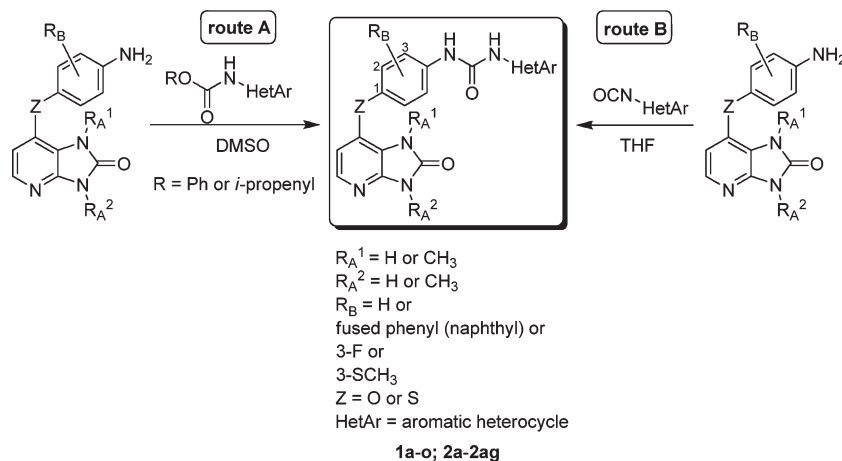
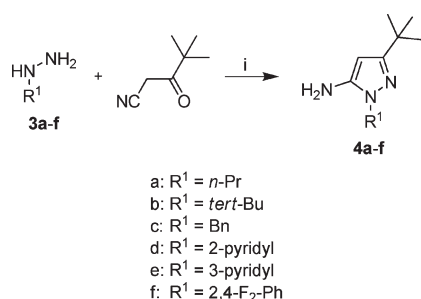
A–B–C) but comprising a 1,3 (meta) substitution of the middle ring B. These derivatives showed an improved selectivity in a panel of kinases; however, the cellular activities remained relatively weak (SRB > 700 nM), the most potent inhibitor being 26 from reference 27 (see Figure 3). Nevertheless, we noticed that some aromatic C-rings (especially substituted pyrazoles) could enhance significantly the cellular potency of these inhibitors.

Therefore, in order to improve the cellular activity of our previous 1,4 (para) substituted B-ring series,²⁶ we set out to optimize the C-ring fragment of the inhibitors focusing on heteroaromatic C-rings. The results of the ensuing structure–activity relationship (SAR) studies are described here.

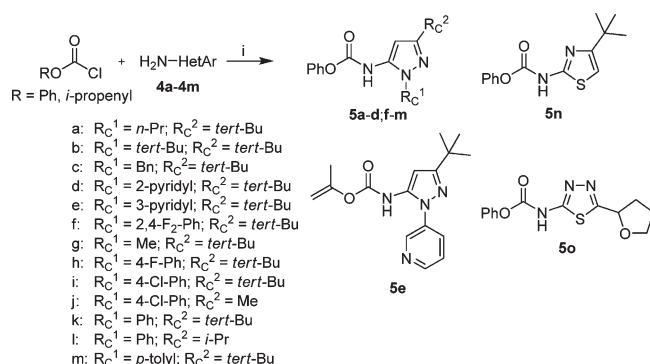
Chemistry

In order to explore the SAR of the C-ring, a synthetic approach was adopted in which the A–B portion was first synthesized and functionalized. The amino group at the B-ring para-position (with respect to the A–B linker) was subsequently reacted with an appropriately activated

Scheme 1. General Synthesis of the BRAF Inhibitors Described in the Current Paper

Scheme 2. Synthesis of 1-Substituted 3-*tert*-Butyl-1*H*-pyrazol-5-amines^{4f}

^a Reagents and conditions: (i) 0.2 M ethanolic HCl or toluene, reflux.

Scheme 3. Synthesis of Activated Carbamates^{4f}

^a Reagents and conditions: (i) pyridine, THF, 0 °C → room temperature.

C-ring fragment to give the target A–B–C system. Thus, the previously described general intermediates^{25–27} were reacted with an aromatic heterocycle functionalized with either an activated carbamate (route A) or an isocyanate group (route B) to give the target compounds (see Scheme 1).

The carbamate functionalized heterocycles (**5a–o**) needed for route A were synthesized in one or two steps, depending on the commercial availability of the required heterocyclic amine. For pyrazolyl amines **4a–f**, the appropriately functionalized hydrazine (**3a–f**) was condensed with 4,4-dimethyl-3-oxopentane nitrile to give the corresponding 1,3-disubstituted-1*H*-pyrazol-5-amines in yields ranging from 27% to quantitative

(see Scheme 2). Compounds **4g–m** are commercially available. The activated carbamates **5a–d** and **5f–o** were subsequently obtained in excellent yields by reacting **4a–d** and **4f–o** with phenyl chloroformate, or in the case of **5e**, **4e** was reacted with isopropenyl chloroformate²⁸ under basic conditions (Scheme 3).

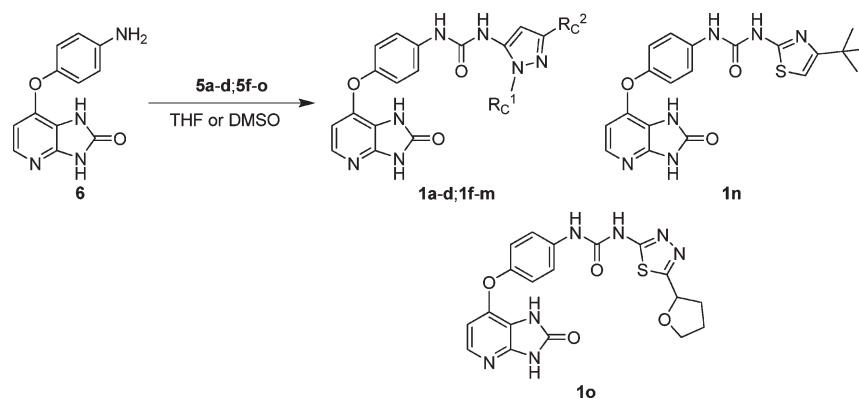
In the final step, **5a–d** and **5f–o** were reacted with general intermediate 7-(4-aminophenoxy)-1*H*-imidazo[4,5-*b*]pyridin-2(3*H*)-one **6** in warm tetrahydrofuran (THF) or in dimethyl sulfoxide (DMSO) to give the corresponding 1-substituted 3-(4-(2-oxo-2,3-dihydro-1*H*-imidazo[4,5-*b*]pyridin-7-yloxy)phenyl)ureas **1a–d** and **1f–o** (Scheme 4, Table 1). This series of compounds, which contain both an unsubstituted 1*H*-imidazo[4,5-*b*]pyridin-2(3*H*)-one ring A and an unsubstituted phenyl ring B, served as a benchmark series to assess the influence of the structural characteristics of ring C on the relative activity of the compounds in the assays.

The C-rings most beneficial for cellular potency found in this study were subsequently connected to a variety of A–B systems^{25–27} via either route A or route B. Route B utilizes functionalized isocyanates for the coupling of the C-ring fragment to an A–B intermediate. The C-ring fragments used here are relatively electron-rich, and the derived isocyanates tend to be less stable, which precludes their commercial availability. Therefore, these isocyanates were prepared from the amine via reaction with phosgene under basic conditions²⁹ and used immediately in the next reaction step. Thus, coupling of a selection of A–B intermediates **7** to C-ring fragments, either by route A or by route B, gave the corresponding urea final compounds **2a–af** in variable yields (see Scheme 5, Table 2, and the Experimental Section).

Selection of C-Ring Fragments

Three *in vitro* assays were used to determine the biological activities of the compounds: (a) IC₅₀ on purified ^{600E}BRAF (IC₅₀, ^{600E}BRAF); (b) IC₅₀ for the inhibition of ERK phosphorylation in mutant BRAF expressing WM266.4 melanoma cells (IC₅₀, pERK); (c) IC₅₀ for proliferation in WM266.4 cells (GI₅₀, SRB). These data are summarized in Tables 1 and 2.

The SAR presented is focused mainly on ring C. Some structural diversity, however, has also been incorporated into the A- and B-ring fragments of some compounds to probe their effects on the activity of these compounds in the *in vitro* assays, as well as their pharmacokinetic (PK) behavior. In Table 1 an overview is presented of the assay results of

Scheme 4. Synthesis of Inhibitors **1a–d** and **1f–o** via Activated Carbamate Route

compounds in which the A-ring (a 7-substituted 1*H*-imidazo[4,5-*b*]pyridin-2(3*H*)-one) and the B-ring (a 1,4-phenylene linker) have been kept constant and in which only the C-ring has been varied (**1a–d**, **f–o**). The C-ring fragments are mainly based on a 1,3-disubstituted-1*H*-pyrazole core which is linked through its 5-position to the B-ring via a urea bridge, which proved essential for the preservation of activity.²⁵

A striking observation from Table 1 is that all C-ring modifications (with the notable exception of di-*tert*-butylpyrazole **1b** and 4-*tert*-butylthiazole **1n**) lead to inhibitors that, in contrast to the previously reported phenyl C-ring compounds,²⁵ exhibit submicromolar potencies on the isolated enzyme. The lower potency of compound **1b** may be explained by its bulky three-dimensional 1-*N-tert*-butylpyrazole substituent. The exploration of the C-ring was initiated because of the difficulty of achieving low nanomolar cellular activities (i.e., in the pERK and SRB assays) with phenyl C-rings.^{25,26} Whereas a number of C-ring modifications do not substantially ameliorate this behavior, the use of a number of 1-aryl-3-*tert*-butylpyrazoles, such as in **1h**, **1i**, **1k**, and **1m**, leads to a significant decrease of the pERK IC₅₀ and SRB GI₅₀ with respect to the previously published phenyl C-ring-containing compounds.^{25,26}

The data in Table 1 indicate that both the 3-*tert*-butyl and 1-aryl substituents are essential for this improvement. Compounds **1a**, **1c**, and **1g** all possess a C-ring 3-*tert*-butyl substituent, but the absence of an aryl group at the pyrazole 1-position renders them only moderately active on cells. Conversely, the drop in cellular potency when going from a 3-*tert*-butyl to a 3-*isopropyl* substituent (cf. **1k** and **1l**) and especially from a 3-*tert*-butyl to a 3-methyl substituent (cf. **1i** and **1j**) supports the assumption that a *tert*-butyl substituent is required at this position for effective cellular potency. A likely explanation is that the change in lipophilicity, due to the presence of the 3-*tert*-butyl group, drives the improvement in cellular activity. In addition, the steric match between the *tert*-butyl group and the kinase's pocket beyond the gatekeeper residue may be of importance, as discussed below.

Variation of the A–B Fragment

A-Ring NH Methylation. After optimizing the C-ring fragment of the inhibitors, we focused on connecting the pyrazole C-ring to the optimized A–B ring fragments described earlier (see Table 2 for synthesized compounds). Methylation at the 1- and 3-positions of the A-ring was performed with the aim of enhancing the PK profile of the compounds by removal of one H-bond donor²⁵ and of investigating whether removal of the NH groups is tolerated.

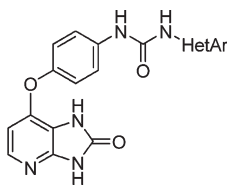
1-Methylated compounds, **2a–g**, generally exhibit good to excellent potencies in all three in vitro assays. For **2a**, **2b**, **2e**, and **2g**, 1-methylation can be directly compared to the corresponding NH analogues **1g**, **1h**, **1k**, and **1m**. Whereas it seems to influence the potency on BRAF only marginally, 1-methylation does have a substantially beneficial impact on the pERK and SRB potencies of **2a**, **2e**, and **2g**. In contrast, 3-methylation has a detrimental effect on the BRAF IC₅₀, which is consistent with the expected result of removing one NH hydrogen bonding interaction with the hinge region of the enzyme.³¹ Recent results, however, imply that these compounds are more potent than suggested by the isolated V^{600E}BRAF enzyme assay.³⁰ Cellular potencies benefit more from 3-methylation than from 1-methylation of the scaffold, whereas this order seems to be reversed for compounds with a naphthyl B-ring. This is consistent with the greater reduction in H-bonding potential through removal of the peripheral 3-NH H-bond donor and the overriding lipophilic contribution to cell penetration provided by the naphthyl group. Interestingly, for the fluoro B-ring series, a change from unmethylated to 1,3-dimethylated does not seem to affect the pERK IC₅₀ values and SRB GI₅₀ values (compare **2y** and **2ab**); it could be hypothesized that the effect on cell permeability of removing one H-bond donor from the imidazopyridinone scaffold is less significant in the case of the fluorophenyl middle ring, which already locks into position one strong H-bond donor of the urea group via an intramolecular H-bond with the halogen atom.

A–B Linker. Substitution of the A–B oxygen linker of **1k** for a sulfur linker to give **2ae** yields a compound that is slightly less potent on the isolated enzyme, but whose cellular activity was improved by a factor of ~10 on pERK and ~30 in the SRB assay, which is likely to be due to the higher lipophilicity of this compound with a concomitant increase in cell permeability. Because of its low solubility in aqueous media, this line of investigation was discontinued.

Improvement of Cellular Potency

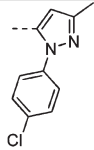
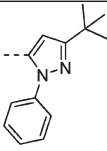
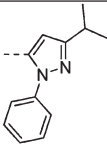
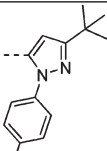
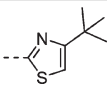
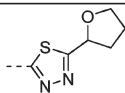
Variations of the B-ring fragment of the inhibitors lead to changes in the BRAF IC₅₀, which have been discussed previously.²⁶ However, it is noteworthy that in the present series similar trends are observed. Thus, all other groups being equal, the potency of the inhibitors increases in the order phenyl < naphthyl ~ 3-F-phenyl < 3-MeS-phenyl.

The potencies of some of the compounds in this paper compared to the corresponding 4-chloro-3-trifluoromethylphenyl C-ring compounds discussed previously^{25,26} are presented in

Table 1. Comparison of the Potencies of Inhibitors with Different C-Rings

| | HetAr | BRAF IC₅₀ (μM) $\pm\text{SEM}$ | pERK IC₅₀ (μM) $\pm\text{SEM}$ | SRB GI₅₀ (μM) (95% CI) |
|-----------|--------------|---|---|---|
| 1a | | 0.083 \pm 0.018 | 10.8 \pm 0.7 | 9.5 (8.7-10.4) |
| 1b | | 1.19 \pm 0.28 | 33 ^a | 26 (23.3-29.3) |
| 1c | | 0.147 \pm 0.004 | 13.4 \pm 4.6 | 10.1 (9.5-10.8) |
| 1d | | 0.21 \pm 0.03 | 6.4 \pm 1.7 | 3.4 (3.2-3.6) |
| 1f | | 0.104 \pm 0.017 | 1.19 \pm 0.23 | 1.23 (1.15-1.32) |
| 1g | | 0.033 \pm 0.006 | 28 ^a | 12.9 (11.8-14.1) |
| 1h | | 0.124 \pm 0.043 | 0.411 \pm 0.046 | 0.54 (0.47-0.62) |
| 1i | | 0.14 \pm 0.03 | 0.35 \pm 0.07 | 0.53 (0.44-0.63) |

Table 1. Continued

| | HetAr | BRAF IC ₅₀ (μ M) \pm SEM | pERK IC ₅₀ (μ M) \pm SEM | SRB GI ₅₀ (μ M) (95% CI) |
|-----------|---|--|--|--|
| 1j |  | 0.29 \pm 0.05 | 70 \pm 17 | 21 (20.0-21.2) |
| 1k |  | 0.094 \pm 0.012 | 0.62 \pm 0.07 | 0.39 (0.34-0.45) |
| 1l |  | 0.042 \pm 0.008 | 1.97 \pm 0.20 | 1.17 (1.05-1.29) |
| 1m |  | 0.142 \pm 0.023 | 0.42 \pm 0.13 | 0.30 (0.25-0.36) |
| 1n |  | 7.8 ^a | n/a | 10.4 (9.4-11.6) |
| 1o |  | 0.17 \pm 0.06 | 58 ^a | 48.9 (45.6-52.5) |

^a Single determination.

Scheme 5. Synthesis of Inhibitors **2a–ag** via Either Activated Carbamate Route A or Isocyanate Route B

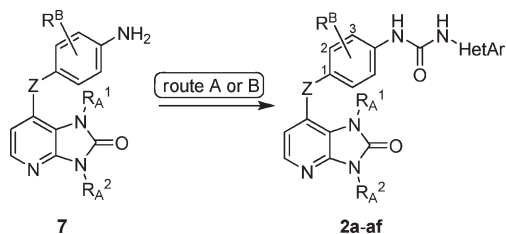


Table 3. In general, these phenylpyrazoles are, according to the CS Chemoffice LogP software, more lipophilic than the analogous compounds with the phenyl C-ring. A striking observation is that C-ring substitution of a 4-chloro-3-trifluoromethylphenyl group by a 3-*tert*-butyl-1-aryl-1*H*-pyrazole (aryl = phenyl or *p*-tolyl) group leads to an increase of potency in the cell-based pERK and the SRB cell proliferation assays. Higher lipophilicity of the latter compounds compared to the former may be a rationale for this behavior, as this is

well-known to enhance passive transport of compounds across the cell membrane. Alternatively, the improvement might be due to the kinetics of binding. In all but one case, the *p*-tolyl-functionalized pyrazole increases the potency more than the phenyl-functionalized pyrazole.

Correlation between pERK IC₅₀ and SRB GI₅₀

A linear regression analysis of the correlation between the pERK IC₅₀ and SRB GI₅₀ data for 39 inhibitors was performed. The analysis yielded a linear relationship between the two variables, expressed as

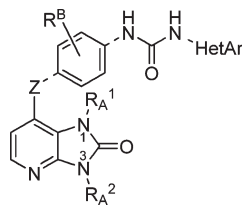
$$SRB = 1.47(pERK) + 1.09 \quad (1)$$

$$n = 39$$

$$s = 2.25 \quad (\text{standard error of the regression model})$$

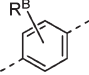
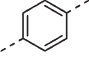
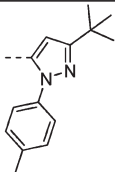
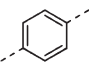
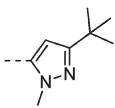
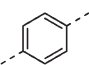
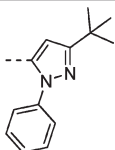
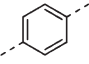
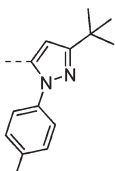
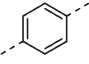
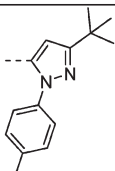
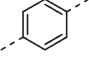
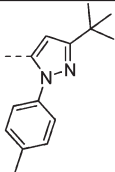
$$F = 4.2 \times 10^{-21} \quad (F \text{ probability of the model})$$

with a regression coefficient r of 0.953 ($r^2 = 0.91$) and a cross-validation index (q^2) of 0.76 (see Figure 4). These data indicate that SRB GI₅₀ and pERK IC₅₀ correlate significantly with a ratio close to unity. This finding provides further evidence for

Table 2. Comparison of the Potencies of Inhibitors with Different Combinations of A-, B-, and C-Rings^a

| | R_A^1 | R_A^2 | Z | R^B | HetAr | BRAF IC ₅₀ (μ M) \pm SEM | pERK IC ₅₀ (μ M) \pm SEM | SRB GI ₅₀ (μ M) (95% CI) |
|-----------|-----------------|---------|---|-------|-------|--|--|--|
| 2a | CH ₃ | H | O | | | 0.084 \pm 0.009 | 14.1 \pm 2.1 | 4.2 (2.3- 7.5) |
| 2b | CH ₃ | H | O | | | 0.135 \pm 0.019 | 1.36 \pm 0.25 | 0.497 (0.45- 0.51) |
| 2c | CH ₃ | H | O | | | 0.176 \pm 0.044 | 3.2 \pm 1.2 | 1.89 (1.67- 2.15) |
| 2d | CH ₃ | H | O | | | 0.143 \pm 0.02 | 18.2 \pm 1.8 | 3.7 (3.57- 3.86) |
| 2e | CH ₃ | H | O | | | 0.215 \pm 0.025 | 0.164 \pm 0.084 | 0.145 (0.135- 0.156) |
| 2f | CH ₃ | H | O | | | 0.39 \pm 0.13 | 0.83 \pm 0.21 | 0.59 (0.56- 0.61) |

Table 2. Continued

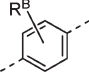
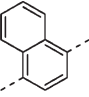
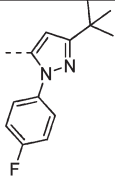
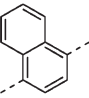
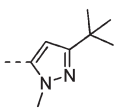
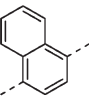
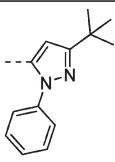
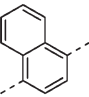
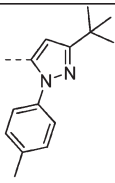
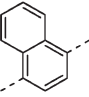
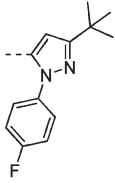
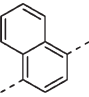
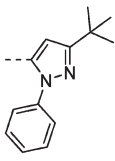
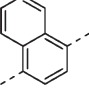
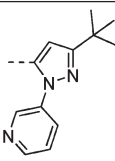
| | R_A^1 | R_A^2 | Z |  | HetAr | BRAF IC ₅₀ (μ M) \pm SEM | pERK IC ₅₀ (μ M) \pm SEM | SRB GI ₅₀ (μ M) (95% CI) |
|-----------|-----------------------------------|-----------------|---|---|---|--|--|--|
| 2g | CH ₃ | H | O |  |  | 0.202 \pm 0.032 | 0.090 \pm 0.016 (0.056- 0.078) | |
| 2h | H | CH ₃ | O |  |  | 0.258 \pm 0.048 | 2.9 \pm 0.1 (1.71- 2.15) | |
| 2i | H | CH ₃ | O |  |  | 0.88 \pm 0.09 | 0.130 \pm 0.031 (0.044- 0.075) | |
| 2j | H | CH ₃ | O |  |  | 1.19 \pm 0.14 | 0.054 \pm 0.023 (0.020- 0.037) | |
| 2k | H. citric acid ^b | CH ₃ | O |  |  | 3.0 \pm 0.7 | 0.036 \pm 0.004 (0.043- 0.061) | |
| 2l | CH ₃ | CH ₃ | O |  |  | 1.8 \pm 0.3 | 0.19 \pm 0.05 (0.18- 0.26) | |

the hypothesis that direct targeting of ^{V600E}BRAF inhibits proliferation of melanoma cells. These findings confirm that this series inhibits cell growth through inhibition of the ERK pathway, which makes the influence of off-pathway effects on proliferation unlikely.

Cellular Selectivity

The SRB GI₅₀ for the BRAF wild-type WM1361 melanoma cell line that does not express mutant BRAF was determined for selected compounds (**1k**, **2r**, **2y**, **2z**) in order to provide evidence for the specificity of the compounds for

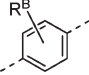
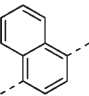
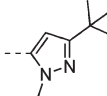
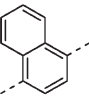
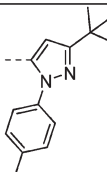
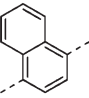
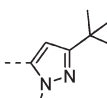
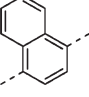
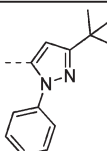
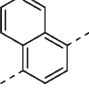
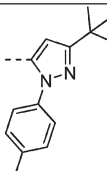
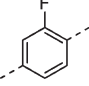
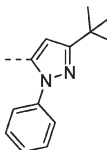
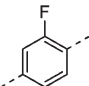
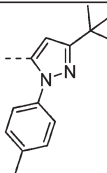
Table 2. Continued

| | R_A^1 | R_A^2 | Z |  | HetAr | BRAF IC ₅₀ (μ M) \pm SEM | pERK IC ₅₀ (μ M) \pm SEM | SRB GI ₅₀ (μ M) (95% CI) |
|-----------|-----------------|---------|---|---|---|--|--|--|
| 2m | H | H | O |  |  | 0.240 \pm 0.015 | 0.203 \pm 0.056 | 0.020 (0.018- 0.022) |
| 2n | H | H | O |  |  | 0.011 \pm 0.002 | 2.3 \pm 0.3 | 0.67 (0.64- 0.70) |
| 2o | H | H | O |  |  | 0.51 \pm 0.22 | 0.035 \pm 0.01 | 0.034 (0.031- 0.039) |
| 2p | H | H | O |  |  | 0.67 \pm 0.13 | 0.014 \pm 0.006 | 0.031 (0.024- 0.041) |
| 2q | CH ₃ | H | O |  |  | 0.313 \pm 0.063 | 0.035 \pm 0.011 | 0.047 (0.041- 0.054) |
| 2r | CH ₃ | H | O |  |  | 0.251 \pm 0.025 | 0.019 \pm 0.002 | 0.024 (0.018- 0.030) |
| 2s | CH ₃ | H | O |  |  | 0.79 \pm 0.31 | 0.100 \pm 0.013 | 0.069 (0.050- 0.094) |

BRAF-driven cell proliferation. The results are shown in Table 4, compared to the SRB GI₅₀ on mutant BRAF

melanoma cell line WM266.4. Unlike sorafenib, for which the activity is independent of BRAF status, these inhibitors

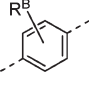
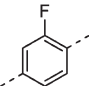
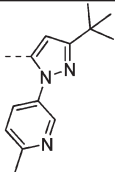
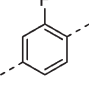
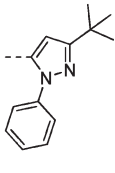
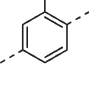
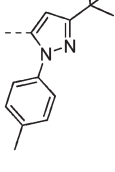
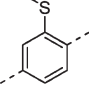
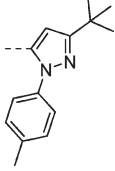
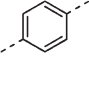
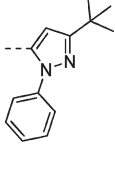
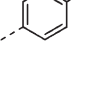
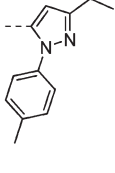
Table 2. Continued

| | R_A^1 | R_A^2 | Z |  | HetAr | BRAF IC ₅₀ (μ M) \pm SEM | pERK IC ₅₀ (μ M) \pm SEM | SRB GI ₅₀ (μ M) (95% CI) |
|----|-----------------|-----------------|---|---|---|--|--|--|
| 2t | CH ₃ | H | O |  |  | 0.099 \pm 0.019 | 0.383 \pm 0.039 | 0.161 (0.148- 0.176) |
| 2u | CH ₃ | H | O |  |  | 2.28 \pm 0.21 | 0.026 \pm 0.012 | 0.016 (0.013- 0.019) |
| 2v | H | CH ₃ | O |  |  | 0.197 \pm 0.030 | 0.47 \pm 0.05 | 0.47 (0.41- 0.54) |
| 2w | H | CH ₃ | O |  |  | 6.9 ^c | 0.027 \pm 0.021 | 0.167 (0.070- 0.402) |
| 2x | H | CH ₃ | O |  |  | 6.3 ^c | 0.070 \pm 0.013 | 1.09 (0.16- 7.13) |
| 2y | H | H | O |  |  | 0.075 \pm 0.019 | 0.135 \pm 0.014 | 0.039 (0.038- 0.041) |
| 2z | H | H | O |  |  | 0.11 \pm 0.005 | 0.04 \pm 0.011 | 0.046 (0.038- 0.055) |

are all selective up to 49-fold for the mutant BRAF WM266.4 cell line. This selectivity strongly supports the proposed

mechanism of action of this series through the inhibition of oncogenic BRAF.

Table 2. Continued

| | R_A^1 | R_A^2 | Z |  | HetAr | BRAF IC ₅₀ (μ M) \pm SEM | pERK IC ₅₀ (μ M) \pm SEM | SRB GI ₅₀ (μ M) (95% CI) |
|------------|-----------------|-----------------|---|---|---|--|--|--|
| 2aa | H | CH ₃ | O |  |  | 0.53 \pm 0.26 | 0.062 \pm 0.011 (0.19- 0.29) | 0.24 (0.19- 0.29) |
| 2ab | CH ₃ | CH ₃ | O |  |  | 1.09 \pm 0.08 | 0.122 \pm 0.02 | 0.033 (0.028- 0.038) |
| 2ac | CH ₃ | CH ₃ | O |  |  | 1.13 \pm 0.13 | 0.052 \pm 0.004 | 0.32 (0.24- 0.43) |
| 2ad | H | H | O |  |  | 0.076 \pm 0.011 | 0.056 \pm 0.008 | 0.016 (0.014- 0.019) |
| 2ae | H | H | S |  |  | 0.215 \pm 0.027 | 0.070 \pm 0.027 | 0.012 (0.011- 0.014) |
| 2af | H | H | S |  |  | 2.2 \pm 1.6 | 0.234 \pm 0.093 | 0.259 (0.208- 0.322) |

^a For a number of compounds (**2j**, **2l**, **2o-r**, **2u**, **2w**, **2x**, **2ab**, **2af**), the BRAF IC₅₀ values are 1–2 orders of magnitude higher than their pERK IC₅₀ and SRB GI₅₀ values. This is due to the short incubation time of the BRAF assay, which is 45 min, compared to the much longer incubation times of the pERK and SRB assays (6 and 96 h, respectively) and not because of the intrinsically lower inhibitory activities of those compounds. ^b Citric acid salt of **2j**. ^c The other two replicates were > 10 μ M.

PK Properties

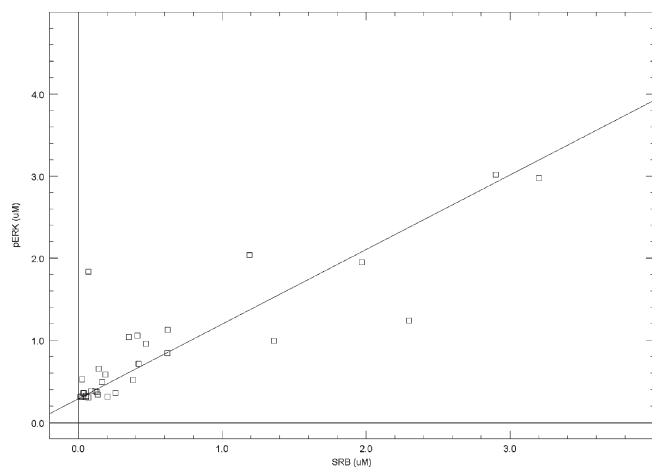
The oral bioavailability (*F*), half-life (*t*_{1/2}), and maximum concentrations of some of the inhibitors were determined in

vivo in BALB/cAnNCrl mice. The results are presented in Table 5. Most of the phenylpyrazole compounds show a significant improvement in *F* compared to the 4-chloro-3-trifluoromethylphenyl C-ring compounds, which generally do

Table 3. Comparison of 4-Chloro-3-trifluoromethylphenyl C-Rings with 3-*tert*-Butyl-1-aryl-1*H*-pyrazole C-Rings

| compd | log <i>P</i> ^a | pERK IC ₅₀ improvement ^b | SRB GI ₅₀ improvement ^b |
|------------|---------------------------|--|---|
| 1k | 4.2 | 3.9 | 11 |
| 1m | 4.7 | 5.7 | 14 |
| 2e | 4.4 | 62 | 37 |
| 2g | 4.9 | 113 | 80 |
| 2i | 4.4 | 116 | 61 |
| 2j | 4.9 | 280 | 137 |
| 2o | 5.2 | 16 | 14 |
| 2p | 5.7 | 40 | 29 |
| 2r | 5.4 | 40 | 43 |
| 2u | 5.9 | 48 | 65 |
| 2w | 5.4 | 116 | 14 |
| 2x | 5.9 | 45 | 2.1 |
| 2y | 4.3 | 16 | 39 |
| 2z | 4.8 | 54 | 33 |
| 2ad | 5.1 | 11 | 29 |

^a Calculated using the ChemDraw LogP function. ^b The reference pERK IC₅₀ or GI₅₀ values are those of analogous 4-chloro-3-trifluoromethylphenyl C-ring compounds with the same A-ring and B-ring as the analogues 3-*tert*-butyl-1-aryl-1*H*-pyrazol-5-yl compounds. The improvement values calculated in this table are the ratio of the pERK IC₅₀ or GI₅₀ values of the 4-chloro-3-trifluoromethylphenyl C-ring compounds to those of the corresponding 3-*tert*-butyl-1-aryl-1*H*-pyrazol-5-yl analogues.

**Figure 4.** Graph showing the correlation between the pERK IC₅₀ and SRB GI₅₀.

not exhibit *F* > 5%. N¹-Methylation seems to be beneficial for the *F* of the compounds (cf. **2g** vs **1m**, respectively). Furthermore, a lipophilic C-ring appears to increase *F* relative to a more polar C-ring (**2r** and **2u** vs **2s**). Metabolism of the compounds by human and mouse liver microsomes is generally low (< 30% at 30 min, data not shown). All compounds reach concentrations well above their GI₅₀ values following oral administration, some greater than 1000-fold. This suggests that effective in vivo concentrations can be easily achieved by oral dosing.

Rationale of Binding

Liao recently published a comprehensive overview of the binding modes of kinase inhibitors to their targets.³² In that context, the structural elements of the inhibitors described here are quite similar to those found in sorafenib and in doramapimod (Figure 1), which bind to the inactive, DFG-out

Table 4. Selectivity of Inhibitors on Wild Type and Mutant BRAF Cell Lines

| compd | SRB GI ₅₀ (μM), WM1361 | SRB GI ₅₀ (μM), WM266.4 | fold difference |
|-----------|-----------------------------------|------------------------------------|-----------------|
| sorafenib | 4.5 | 5.2 | 1 |
| 1k | 3.2 | 0.39 | 8 |
| 2r | 1.2 | 0.024 | 49 |
| 2y | 0.66 | 0.039 | 17 |
| 2z | 0.79 | 0.046 | 17 |

Table 5. Pharmacokinetic Data for Selected Compounds, Based on Plasma Levels after a 10 mg/kg Single Dose po

| compd ^a | <i>F</i> (%) | <i>t</i> _{1/2} (h) ^b | max concn (nM) ^c |
|------------------------|--------------|--|-----------------------------|
| 1m ^d | 6.5 | 4.0 (15) | 3674 (0.5, 12) |
| 2g | 34 | 3.4 (24) | 39594 (1, 600) |
| 2j | 30 | 3.4 (24) | 22675 (1, 840) |
| 2r ^d | 33 | 1.91 (20.5) | 35492 (1.5, 1480) |
| 2s | 5 | 0.8 (5) | 4207 (0.5, 60) |
| 2u | 43 | 8.4 (24) | 43320 (1, 2700) |
| 2y | 24 | 2.8 (19) | 15020 (0.25, 390) |
| 2z | 7 | 5.3 (24) | 7425 (1.5, 160) |
| 2aa | 17 | 12.6 (> 6) | 18024 (0.25, 1060) |
| 2ab | 59 | 2.1 (18) | 4444 (0.5, 135) |
| 2ac | 31 | 9.4 (> 18) | 8120 (0.5, 226) |

^a 10 mg/kg single dose po unless otherwise noted. ^b In parentheses the number of hours the concentration of a compound is above its GI₅₀ after oral administration. ^c In parentheses the *t*_{max} (h) and the ratio between the plasma concentration of compound and its GI₅₀ at *t*_{max} after oral administration. ^d 20 mg/kg single dose po.

conformation of the BRAF and p38α proteins, respectively, and are thus classified as type II kinase inhibitors.³³ On the basis of this rationale, we propose a tentative binding mode of the inhibitors described here, which is depicted in Figure 5. Within this model, the A-ring fragment of the inhibitor (as exemplified here by **1m**) forms a hydrogen bond with the hinge region of the kinase through its pyridine nitrogen atom, possibly in conjunction with its ortho imidazolone proton. This fragment is connected through the 1,4-phenylene or -naphthalene bridge to the urea part, which forms a network of hydrogen bonds with the enzyme. As in the structure of doramapimod with p38 MAP kinase, the *p*-tolyl part of the pyrazolyl fragment probably protrudes through the BP-IV pocket into the E₂ binding pocket (nomenclature adopted from Liao).³² In contrast, its *tert*-butyl substituent fills the hydrophobic BP-III pocket in a similar way as the C-ring CF₃ group of sorafenib does in BRAF. The docking of compound **2y** on the sorafenib/BRAF cocrystal structure (PDB code UWH)⁵ confirms this model. The docking pose showing selected amino acids and key ligand-protein interactions is presented in Figure 6. As expected, the binding mode is reminiscent of that of sorafenib, with the pyridoimidazolone unit forming a hydrogen bond with the backbone of Cys532 of the hinge region. Three more H bonds are formed by the urea moiety of the inhibitor, two between the NH groups and the Glu501 side chain and one between the carbonyl moiety and the backbone of Asp594 of the DFG motif. Notably, the fluoro atom on the B ring of **2y** elaborates into the BPI cavity of BRAF, which is not occupied by sorafenib, while the *tert*-butylpyrazole of the C ring of **2y** forms extensive interactions with the kinase pocket beyond the gatekeeper residue, in particular between the *tert*-butyl group and the BPIII pocket.

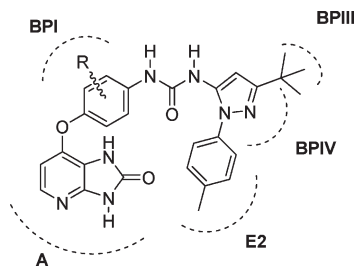


Figure 5. Proposed binding mode of **1m** to BRAF.

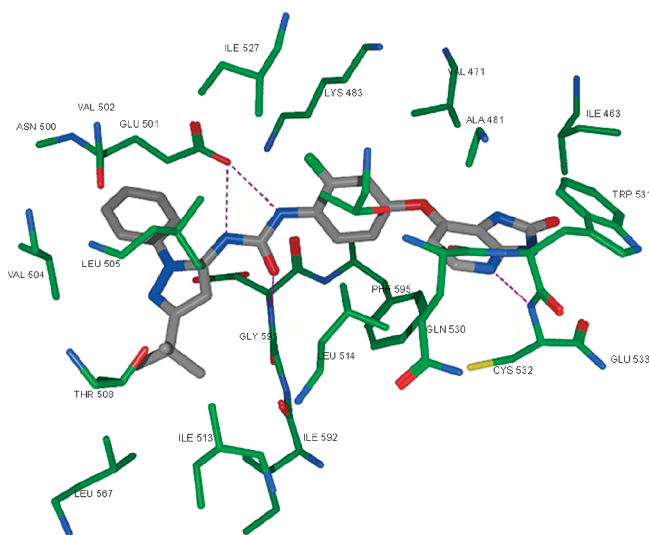


Figure 6. Docking pose of compound **2y** into the sorafenib-BRAF cocrystal structure.

Conclusions

Building on the knowledge and insights gained from previous studies, a series has been synthesized. These are based on a 7-aryloxy-1*H*-imidazo[4,5-*b*]pyridin-2(3*H*)-one scaffold that is linked to an aromatic heterocyclic fragment (ring C) via a urea bridge. The use of 3-*tert*-butyl-1-aryl-1*H*-pyrazoles instead of the previously used substituted phenyl groups as C-rings led to a marked improvement in cellular potency *in vitro*, while modifications on the rest of the scaffold enhanced PK properties such as oral bioavailability and half-life *in vivo*. Seven compounds have oral bioavailabilities of $\geq 30\%$ up to 59% for **2ab**. This illustrates that these inhibitors can reach effective *in vivo* concentrations following oral administration, and their further investigation *in vivo* in xenograft models is warranted.

Experimental section

Materials and Methods. Starting materials, reagents, and solvents for reactions were reagent grade and used as purchased. 7-(4-Aminophenoxy)-1*H*-imidazo[4,5-*b*]pyridin-2(3*H*)-one **6**,²⁵ 7-(4-aminophenoxy)-1-methyl-1*H*-imidazo[4,5-*b*]pyridin-2(3*H*)-one, 7-(4-aminophenoxy)-3-methyl-1*H*-imidazo[4,5-*b*]pyridin-2(3*H*)-one,²⁵ 7-(4-aminophenoxy)-1,3-dimethyl-1*H*-imidazo[4,5-*b*]pyridin-2(3*H*)-one,²⁵ 7-(4-aminonaphthalen-1-yloxy)-1*H*-imidazo[4,5-*b*]pyridin-2(3*H*)-one,²⁶ 7-(4-aminonaphthalen-1-yloxy)-1-methyl-1*H*-imidazo[4,5-*b*]pyridin-2(3*H*)-one,²⁶ 7-(4-aminonaphthalen-1-yloxy)-3-methyl-1*H*-imidazo[4,5-*b*]pyridin-2(3*H*)-one,²⁶ 7-(4-amino-3-fluorophenoxy)-1*H*-imidazo[4,5-*b*]pyridin-2(3*H*)-one,²⁶ 7-(4-amino-3-(methylthio)phenoxy)-1*H*-imidazo[4,5-*b*]pyridin-2(3*H*)-one,²⁶ and 7-(4-aminophenylthio)-1*H*-imidazo[4,5-*b*]pyridin-2(3*H*)-one²⁵ were synthesized according to described

procedures. Chromatography solvents were HPLC grade and were used without further purification. Reactions were monitored by thin layer chromatography (TLC) analysis using Merck silica gel 60 F-254 thin layer plates. Flash column chromatography was carried out on Merck silica gel 60 (0.015–0.040 mm) or in disposable Isolute Flash Si and Si II silica gel columns. Preparative TLC was performed on either Macherey-Nagel [809 023] precoated TLC plates SIL G-25 UV₂₅₄ or Analtech [2015] precoated preparative TLC plates, 2000 μm with UV₂₅₄. LCMS analyses were performed on a Micromass LCT/Water's Alliance 2795 HPLC system with a Discovery 5 μm , C18, 50 mm \times 4.6 mm i.d. column from Supelco at 22 °C using the following solvent systems: solvent A (methanol) and solvent B (0.1% formic acid in water) at a flow rate of 1 mL/min. The gradient started with 10% A/90% B from 0 to 0.5 min and then 10% A/90% B to 90% A/10% B from 0.5 to 6.5 min and continuing at 90% A/10% B up to 10 min. From 10 to 10.5 min the gradient reverted back to 10% A/90% B where the concentrations remained until 12 min. UV detection was at 254 nm, and ionization was positive or negative ion electrospray. The molecular weight scan range was 50–1000. Samples were supplied as 1 mg/mL in DMSO or methanol with 3 μL injected on a partial loop fill. NMR spectra were recorded in DMSO-*d*₆ on a Bruker DPX 250 MHz or a Bruker Advance 500 MHz spectrometer. Chemical shifts (δ) are given in ppm and are referenced to residual, not fully deuterated, solvent signal (i.e., DMSO-*d*₅). Coupling constants (*J*) are given in Hz. HRMS analyses were performed on an Agilent 6210 time of flight mass spectrometer with an Agilent 1200 series HPLC system. The internal references were caffeine ($[\text{M} + \text{H}]^+$ 195.087 652), reserpine ($[\text{M} + \text{H}]^+$ 609.280 657) and (1*H*,1*H*,3*H*-tetrafluoropentoxo)phosphazene ($[\text{M} + \text{H}]^+$ 922.009 798). The mobile phase consisted of 0.1% formic acid in doubly distilled deionized water (solvent A) and HPLC-grade methanol (solvent B) with all runs executed at 1.0 mL/min flow rate. For condition A, the column Restek Ultra Aqueous 3 μm C18 (30 mm \times 4.6 mm i.d.) was used with a gradient starting at 90:10 (A/B) from 0.0 to 0.2 min, then 90:10 to 10:90 from 0.2 to 4.0 min, and continuing at 10:90 from 4.0 to 9.25 min before reverting back to 90:10 at 10 min. The purities of the final compounds described here were determined by HPLC as described above and are 95% or higher unless stated otherwise.

Linear regression analysis was carried out using TSAR 3.3 (Accelrys Inc., San Diego, CA). Docking studies were performed using GOLD,³⁴ version 3.1. Partial charges of the ligand were derived using the Charge-2 CORINA 3D package in TSAR 3.3, and its geometry was optimized using the COSMIC module of TSAR. The calculations were terminated if the energy difference or the energy gradient were smaller than 1×10^{-5} kJ. Ten docking solutions were generated in the docking run, and the best three were stored for analysis.

General Methods and Examples for the Synthesis of Inhibitors 1a–o and 2a–af. Route A1. A mixture of the appropriate phenyl carbamate and substituted aniline in anhydrous THF with or without 4 Å molecular sieves was heated for the stated amount of time. After dilution with EtOAc and filtration, the solution was washed with 0.5 M citric acid(aq), saturated NaHCO₃(aq), and brine. The organic layer was dried over MgSO₄ and filtered, and the solvent was evaporated under reduced pressure. The residue was finally washed with Et₂O to afford the title compound as a solid.

1-(3-*tert*-Butyl-1-phenyl-1*H*-pyrazol-5-yl)-3-(4-(2-oxo-2,3-dihydro-1*H*-imidazo[4,5-*b*]pyridin-7-yloxy)phenyl)urea (1k**).** Route A1 was employed, using **5k** (97 mg, 0.29 mmol) and **6** (50 mg, 0.20 mmol) with 4 Å molecular sieves at 50 °C for 17 h. The title compound was obtained as a slightly orange solid (43 mg, 45%). ¹H NMR, δ : 1.28 (s, 9H, *tert*-Bu), 6.32 (d, 1H, *J* = 6.0, H_{Py,5}), 6.37 (s, 1H, H_{Py,4}), 7.10 (d, 2H, *J* = 9.0, H_{arom,Ph,3+5}), 7.37–7.54 (m, 5H, H_{arom,Ph-Pyz}), 7.47 (d, 2H, *J* = 9.0, H_{arom,Ph,2+6}), 7.75 (d, 1H, *J* = 6.0, H_{Py,6}), 8.40 (bs, 1H, NH_{urea}), 9.11 (bs, 1H, NH_{urea}), 11.16

(bs, 1H, NH_{Py3}), 11.34 (bs, 1H, NH_{Py2}). ¹³C NMR, δ: 30.1, 32.0, 95.6, 105.2, 112.8, 119.7, 120.4, 124.2, 127.2, 129.2, 136.4, 137.0, 138.5, 141.2, 145.8, 146.8, 148.5, 151.5, 154.1, 160.7. LC-MS: *m/z* 484 ([M + H]⁺, 100). HRMS (EI): *m/z* calcd for C₂₆H₂₆N₇O₃ ([M + H]⁺), 484.2097; found, 484.2101.

1-(3-*tert*-Butyl-1-(4-fluorophenyl)-1*H*-pyrazol-5-yl)-3-(4-(2-oxo-2,3-dihydro-1*H*-imidazo[4,5-*b*]pyridin-7-yl-oxy)naphthalen-1-yl)urea (2m). Route A1 was employed, using **5h** (50 mg, 0.15 mmol) and 7-(4-aminonaphthalen-1-yloxy)-1*H*-imidazo[4,5-*b*]pyridin-2(3*H*)-one (29 mg, 0.10 mmol) with 4 Å molecular sieves at 50 °C for 17 h. The title compound was obtained as a brown solid (12 mg, 22%). ¹H NMR, δ: 1.35 (s, 9H, *tert*-Bu), 6.20 (d, 1H, *J* = 6.0, H_{Py,5}), 6.40 (s, 1H, H_{Py,4}), 7.29 (d, 2H, *J* = 8.5, H_{arom,Naph}), 7.41 (t, 2H, *J* = 8.5, H_{arom,4-F-Ph,3+5}), 7.58–7.70 (m, 5H, H_{arom,Naph+4-F-Ph}), 7.87 (d, 1H, *J* = 8.5, H_{arom,Naph}), 7.94 (d, 1H, *J* = 8.5, H_{arom,Naph}), 8.05 (d, 1H, *J* = 6.0 H_{Py,6}), 8.76 (s, 1H, NH_{urea}), 9.06 (s, 1H, NH_{urea}), 11.37 (bs, 1H, NH_{Py3}), 11.43 (bs, 1H, NH_{Py2}). LC-MS: *R_f* = 7.62 min; *m/z* 552.2 ([M + H]⁺, 100). HRMS (EI): *m/z* calcd for C₂₅H₂₆N₇O₃ ([M + H]⁺), 552.2159; found, 552.2164.

Route A2. A solution of the appropriate phenyl carbamate and substituted aniline in anhydrous DMSO with or without 4 Å molecular sieves was heated for the stated amount of time. After cooling to room temperature, the solution was diluted in EtOAc, washed twice with H₂O, and washed once with brine. The organic layer was dried over MgSO₄ and filtered, and the solvent was evaporated under reduced pressure. The solid residue was washed with Et₂O to afford the title compound.

1-(3-*tert*-Butyl-1-*p*-tolyl-1*H*-pyrazol-5-yl)-3-(4-(2-oxo-2,3-dihydro-1*H*-imidazo[4,5-*b*]pyridin-7-yloxy)phenyl)urea (1m). Route A2 was employed, using **5m** (53 mg, 0.15 mmol) and **6** (30 mg, 0.12 mmol) at 55 °C for 3.5 h. The title compound was obtained as an off-white solid (40 mg, 67%). ¹H NMR, δ: 1.27 (s, 9H, *tert*-Bu), 2.37 (s, 3H, CH₃Ph), 6.31 (d, 1H, *J* = 6.0, H_{Py,5}), 6.34 (s, 1H, H_{Py,4}), 7.09 (d, 2H, *J* = 8.9, H_{arom,Ph,3+5}), 7.33 (d, 2H, *J* = 8.4, H_{arom,p-tol}), 7.40 (d, 2H, *J* = 8.4, H_{arom,p-tol}), 7.47 (d, 2H, *J* = 8.9, H_{arom,Ph,2+6}), 7.74 (d, 1H, *J* = 6.0, H_{Py,6}), 8.38 (bs, 1H, NH_{urea}), 9.14 (bs, 1H, NH_{urea}), 11.16 (bs, 1H, NH_{Py3}), 11.34 (bs, 1H, NH_{Py2}). ¹³C NMR, δ: 20.4, 30.0, 31.8, 95.2, 105.2, 112.8, 119.6, 120.3, 124.1, 129.5, 136.0, 136.4, 136.5, 136.9, 141.1, 145.7, 146.8, 148.5, 151.5, 154.0, 160.3. LC-MS: *m/z* 498 ([M + H]⁺, 100). HRMS (EI): *m/z* calcd for C₂₇H₂₈N₇O₃ ([M + H]⁺), 498.2254; found, 498.2234.

1-[1-*N*-(4-Fluorophenyl)-3-*tert*-butylpyrazol-5-yl]-3-(4-(2-oxo-2,3-dihydro-1-*N*-methyl-1*H*-imidazo[4,5-*b*]pyridin-7-yl-oxy)naphthalen-1-yl)urea (2q). Route A2 was employed, using **5h** (177 mg, 0.5 mmol) and 7-(4-aminonaphthalen-1-yloxy)-1-*N*-methyl-1*H*-imidazo[4,5-*b*]pyridin-2(3*H*)-one (100 mg, 0.33 mmol) at 42 °C for 18 h. The title compound was obtained as an off-white solid (130 mg, 70%). Purity: 76%. ¹H NMR, δ: 1.28 (s, 9H, *tert*-Bu), 3.53 (s, 3H, CH₃), 6.29 (d, 1H, *J* = 6.0, H_{Py,5}), 6.39 (s, 1H, H_{Py,4}), 7.24 (d, 1H, *J* = 8.3, H_{arom}), 7.32 (t, 1H, *J* = 8.8, H_{arom}), 7.39 (t, 2H, *J* = 8.8, H_{arom}), 7.60–7.66 (m, 3H, H_{arom}), 7.73 (d, 1H, *J* = 6.0, H_{Py,6}), 7.84 (d, 1H, *J* = 8.3, H_{arom}), 8.06 (d, 1H, *J* = 8.9, H_{arom}), 8.08 (d, 1H, *J* = 8.8, H_{arom}), 8.72 (s, 1H, NH_{urea}), 9.02 (s, 1H, NH_{urea}), 11.65 (s, 1H, NH_{Py3}). LC-MS: *R_f* = 7.94 min; *m/z* 566.2 ([M + H]⁺, 100). HRMS (EI): *m/z* calcd for C₃₁H₂₇FN₇O₃ ([M + H]⁺), 566.2316; found, 566.2314.

Route B. The appropriate pyrazolyl-5-amine was dissolved in a volume of CH₂Cl₂ (~50 mM), and an equal volume of saturated NaHCO_{3(aq)} was added. The biphasic mixture was stirred and cooled to 0 °C with an ice/water bath. After 10 min, 2 equiv of phosgene (1.9 M solution in toluene) were added. The mixture was vigorously stirred for 10 min, the organic layer was isolated, washed with H₂O, dried (MgSO₄), and concentrated to about 100 mM. This solution (1–2 equiv) was added to a solution of the appropriate amine in THF. The solution was stirred for a given amount of time at room temperature, the solvents were evaporated, and the solid residue was washed with Et₂O to afford the title compound.

1-(1-*N*-*p*-Tolyl-3-*tert*-butylpyrazol-5-yl)-3-(4-(2-oxo-2,3-dihydro-1*H*-imidazo[4,5-*b*]pyridin-7-yl-oxy)naphthalen-1-yl)urea (2p). Route B was employed, using **4m** (40 mg, 0.17 mmol) and 7-(4-aminonaphthalen-1-yloxy)-1*H*-imidazo[4,5-*b*]pyridin-2(3*H*)-one (40 mg, 0.13 mmol) for 14 h. The title compound was obtained as an off-white solid (66 mg, 93%). Purity: 96%. ¹H NMR, δ: 1.28 (s, 9H, *tert*-Bu), 2.40 (s, 3H, CH₃), 6.21 (d, 1H, *J* = 5.9, H_{Py,5}), 6.39 (s, 1H, H_{Py,4}), 7.27 (d, 1H, *J* = 8.3, H_{arom}), 7.37 (d, 2H, *J* = 8.1, H_{arom}), 7.45 (d, 2H, *J* = 8.3, H_{arom}), 7.59 (t, 1H, *J* = 7.6, H_{arom}), 7.64 (t, 1H, *J* = 7.0, H_{arom}), 7.69 (d, 1H, *J* = 5.9, H_{Py,6}), 7.89 (d, 1H, *J* = 8.3, H_{arom}), 7.95 (d, 1H, *J* = 8.3, H_{arom}), 8.07 (d, 1H, *J* = 8.5, H_{arom}), 8.72 (s, 1H, NH_{urea}), 9.06 (s, 1H, NH_{urea}), 11.32 (s, 1H, NH_{Py2}), 11.38 (s, 1H, NH_{Py3}). LC-MS: *R_f* = 5.05 min; *m/z* 547.2 (M⁺, 100). HRMS (EI): *m/z* calcd for C₃₁H₃₀N₇O₃ ([M + H]⁺), 548.2405; found, 548.2410.

1-(1-*N*-*p*-Tolyl-3-*tert*-butylpyrazol-5-yl)-3-(4-(2-oxo-2,3-dihydro-1-*N*-methyl-1*H*-imidazo[4,5-*b*]pyridin-7-yl-oxy)naphthalen-1-yl)urea (2u). Route B was employed, using **4m** (35 mg, 0.15 mmol) and 7-(4-aminonaphthalen-1-yloxy)-1-*N*-methyl-1*H*-imidazo[4,5-*b*]pyridin-2(3*H*)-one (40 mg, 0.13 mmol) for 14 h. The title compound was obtained as an off-white solid (52 mg, 71%). Purity: 84%. ¹H NMR, δ: 1.28 (s, 9H, *tert*-Bu), 2.40 (s, 3H, CH₃), 3.53 (s, 3H, CH₃), 6.29 (d, 1H, *J* = 5.9, H_{Py,5}), 6.39 (s, 1H, H_{Py,4}), 7.24 (d, 1H, *J* = 8.4, H_{arom}), 7.36 (d, 2H, *J* = 8.2, H_{arom}), 7.45 (d, 2H, *J* = 8.2, H_{arom}), 7.60 (t, 1H, *J* = 7.5, H_{arom}), 7.67 (t, 1H, *J* = 7.6, H_{arom}), 7.74 (d, 1H, *J* = 5.9, H_{Py,6}), 7.87 (d, 1H, *J* = 8.3, H_{arom}), 8.07 (d, 2H, *J* = 8.3, H_{arom}), 8.71 (s, 1H, NH_{urea}), 9.06 (s, 1H, NH_{urea}), 11.65 (s, 1H, NH_{Py3}). LC-MS: *R_f* = 5. min; *m/z* 562.2 ([M + H]⁺, 100). HRMS (EI): *m/z* calcd for C₃₂H₃₂N₇O₃ ([M + H]⁺), 562.2561; found, 562.2566.

Biological Assays. ^{V600E}**BRAF Kinase Assay and SRB IC₅₀ for BRAF Inhibitors.** These assays have been described by Niculescu-Duvaz et al.²³ BRAF assays were performed in triplicate for each compound except for compound **1n** for which a single measurement was performed. The SRB assays were performed in quadruplicate.

pERK Kinase Assay. This assay has been described by Ménard et al.²⁶ and was performed in triplicate except for compounds **1b**, **1g**, **1o**, which are single measurements.

Compound Metabolism. Microsomal incubations evaluating phase I metabolism were performed as previously described.³⁵ Compounds were incubated at 10 μM for 30 min. The reaction was stopped by the addition of methanol (3 volumes), containing roscovitine (500 nM) used as an internal standard. The parent compound and metabolites were measured by liquid chromatography–mass spectrometry with electrospray in positive ionization mode on two instruments as previously described.³⁶ The chromatographic separation was achieved on a Synergi polar RP column (5 cm, 4 μm particle, 4.6 mm i.d.; Phenomenex, Cheshire, U.K.) with gradient and mass spectrometry conditions similar to those described by Nutley et al.³⁶

Pharmacokinetics. Female BALB/cAnNCrl mice at least 6 weeks of age were used for the PK analyses except for the intravenous administration of **1m**, which was carried out with female Crl:CD1-Foxn1nu mice bearing V600E mutant BRAF WM266.4 tumor xenografts. The mice were dosed intravenously (2 mg/kg, equivalent to ~4 μmol/kg, 10 mL/kg, in DMSO/Tween-20/water, 10:1:89 v/v/v) or orally by gavage (10 mg/kg, equivalent to ~20 μmol/kg except for **2r** whose dosage was 20 mg/kg, 10 mL/kg, in DMSO/water, 1:19 v/v). Samples were taken at seven or eight time points between 5 min and 18 or 24 h for the intravenous route and at six or eight time points between 15 min and 18 or 24 h for the oral route. Three mice were used per time point per route. They were placed under halothane or isoflurane anesthesia, and blood for plasma preparation was taken by terminal cardiac puncture into heparinized syringes. Plasma samples were snap frozen in liquid nitrogen and then stored at –70 °C prior to analysis. All procedures involving animals were performed in accordance with national Home Office regulations under the

Animals (Scientific Procedures) Act 1986 and within guidelines set out by the Institute's Animal Ethics Committee and the United Kingdom Coordinating Committee for Cancer Research's Ad Hoc Committee on the Welfare of Animals in Experimental Neoplasia.³⁷

Acknowledgment. We thank Cancer Research UK (Grants C309/A8274 and C107/A10433), the Wellcome Trust, the Institute of Cancer Research, and the Isle of Man Anti-Cancer Association for funding. We are grateful to Neus Cantarino, Meirion Richards, and Dr. Amin Mirza for providing technical assistance and to Professors Julian Blagg and Paul Workman for suggestions, support, and helpful comments.

Supporting Information Available: Synthetic details and characterization data for **4a–f**, **5a–o**, **1a–j,l,n,o**, and **2a–l,n,o,r–t,v–z,aa–af**. This material is available free of charge via the Internet at <http://pubs.acs.org>.

References

- Weinberg, R. A. *The Biology of Cancer*; Garland Science, Taylor & Francis Group, LLC: New York, 2007; pp 173–176.
- Dhillon, A. S.; Hagan, S.; Rath, O.; Kolch, W. MAP kinase signalling pathways in cancer. *Oncogene* **2007**, *26* (22), 3279–3290.
- Davies, H.; Bignell, G. R.; Cox, C.; Stephens, P.; Edkins, S.; Clegg, S.; Teague, J.; Woffendin, H.; Garnett, M. J.; Bottomley, W.; Davis, N.; Dicks, N.; Ewing, R.; Floyd, Y.; Gray, K.; Hall, S.; Hawes, R.; Hughes, J.; Kosmidou, V.; Menzies, A.; Mould, C.; Parker, A.; Stevens, C.; Watt, S.; Hooper, S.; Wilson, R.; Jayatilake, H.; Gusterson, B. A.; Cooper, C.; Shiple, J.; Hargrave, D.; Pritchard-Jones, K.; Maitland, N.; Chenevix-Trench, G.; Riggins, G. J.; Bigner, D. D.; Palmieri, G.; Cossu, A.; Flanagan, A.; Nicholson, A.; Ho, J. W. C.; Leung, S. Y.; Yuen, S. T.; Weber, B. L.; Siegler, H. F.; Darrow, T. L.; Paterson, H.; Marais, R.; Marshall, C. J.; Wooster, R.; Stratton, M. R.; Futreal, P. A. Mutations of the BRAF gene in human cancer. *Nature* **2002**, *417* (6892), 949–954.
- Gray-Schopfer, V.; Wellbrock, C.; Marais, R. Melanoma biology and new targeted therapy. *Nature* **2007**, *445* (7130), 851–857.
- Wan, P. T. C.; Garnett, M. J.; Roe, S. M.; Lee, S.; Niculescu-Duvaz, D.; Good, V. M.; Jones, C. M.; Marshall, C. J.; Springer, C. J.; Barford, D.; Marais, R.; Cancer Genome Project. Mechanism of activation of the RAF-ERK signaling pathway by oncogenic mutations of B-RAF. *Cell* **2004**, *116* (6), 855–867.
- Dhanasekaran, D. N.; Johnson, G. L. MAPKs: function, regulation, role in cancer and therapeutic targeting. *Oncogene* **2007**, *26* (22), 3097–3099.
- Sebolt-Leopold, J. S. Development of anticancer drugs targeting the MAP kinase pathway. *Oncogene* **2000**, *19* (56), 6594–6599.
- Sebolt-Leopold, J. S.; Herrera, R. Targeting the mitogen-activated protein kinase cascade to treat cancer. *Nat. Rev. Cancer* **2004**, *4* (12), 937–947.
- Karasarides, M.; Chilocheas, A.; Hayward, R.; Niculescu-Duvaz, D.; Scanlon, I.; Friedlos, F.; Ogilvie, L.; Hedley, D.; Martin, J.; Marshall, C. J.; Springer, C. J.; Marais, R. B-RAF is a therapeutic target in melanoma. *Oncogene* **2004**, *23* (37), 6292–6298.
- Roberts, P. J.; Der, C. J. Targeting the Raf-MEK-ERK mitogen-activated protein kinase cascade for the treatment of cancer. *Oncogene* **2007**, *26* (22), 3291–3310.
- Sebolt-Leopold, J. S. Advances in the development of cancer therapeutics directed against the RAS-mitogen-activated protein kinase pathway. *Clin. Cancer Res.* **2008**, *14* (12), 3651–3656.
- Khazak, V.; Astsaturov, I.; Serebriiskii, I. G.; Golemis, E. A. Selective Raf inhibition in cancer therapy. *Expert Opin. Ther. Targets* **2007**, *11* (12), 1587–1609.
- Lowinger, T. B.; Riedl, B.; Dumas, J.; Smith, R. A. Design and discovery of small molecules targeting Raf-1 kinase. *Curr. Pharm. Des.* **2002**, *8* (25), 2269–2278.
- Wilhelm, S.; Carter, C.; Lynch, M.; Lowinger, T.; Dumas, J.; Smith, R. A.; Schwartz, B.; Simantov, R.; Kelley, S. Discovery and development of sorafenib: a multikinase inhibitor for treating cancer. *Nat. Rev. Drug Discovery* **2006**, *5* (10), 835–844.
- Barker, A. J.; Gibson, K. H.; Grundy, W.; Godfrey, A. A.; Barlow, J. J.; Healy, M. P.; Woodburn, J. R.; Ashton, S. E.; Curry, B. J.; Scarlett, L.; Henthorn, L.; Richards, L. Studies leading to the identification of ZD1839 (Iressa): an orally active, selective epidermal growth factor receptor tyrosine kinase inhibitor targeted to the treatment of cancer. *Bioorg. Med. Chem. Lett.* **2001**, *11* (14), 1911–1914.
- Druker, B. J.; Tamura, S.; Buchdunger, E.; Ohno, S.; Segal, G. M.; Fanning, S.; Zimmermann, J.; Lydon, N. B. Effects of a selective inhibitor of the Abl tyrosine kinase on the growth of Bcr-Abl positive cells. *Nat. Med.* **1996**, *2* (5), 561–566.
- Zimmermann, J.; Buchdunger, E.; Mett, H.; Meyer, T.; Lydon, N. B. Potent and selective inhibitors of the Abl-kinase: phenylamino-pyrimidine (PAP) derivatives. *Bioorg. Med. Chem. Lett.* **1997**, *7* (2), 187–192.
- Capdeville, R.; Buchdunger, E.; Zimmermann, J.; Matter, A. Glivec (ST1571, imatinib), a rationally developed, targeted anti-cancer drug. *Nat. Rev. Drug Discovery* **2002**, *1* (7), 493–502.
- Moyer, J. D.; Barbacci, E. G.; Iwata, K. K.; Arnold, L.; Boman, B.; Cunningham, A.; DiOrto, C.; Doty, J.; Morin, M. J.; Moyer, M. P.; Neveu, M.; Pollack, V. A.; Pustilnik, L. R.; Reynolds, M. M.; Sloan, D.; Theleman, A.; Miller, P. Induction of apoptosis and cell cycle arrest by CP-358,774, an inhibitor of epidermal growth factor receptor tyrosine kinase. *Cancer Res.* **1997**, *57* (21), 4838–4848.
- Sun, L.; Liang, C.; Shirazian, S.; Zhou, Y.; Miller, T.; Cui, J.; Fukuda, J. Y.; Chu, J. Y.; Nematalla, A.; Wang, X.; Chen, H.; Sistla, A.; Luu, T. C.; Tang, F.; Wei, J.; Tang, C. Discovery of 5-[5-fluoro-2-oxo-1,2-dihydroindol-(3Z)-ylidenemethyl]-2,4-dimethyl-1H-pyrrole-3-carboxylic acid (2-diethylaminoethyl)amide, a novel tyrosine kinase inhibitor targeting vascular endothelial and platelet-derived growth factor receptor tyrosine kinase. *J. Med. Chem.* **2003**, *46* (7), 1116–1119.
- Lombardo, L. J.; Lee, F. Y.; Chen, P.; Norris, D.; Barrish, J. C.; Behnia, K.; Castaneda, S.; Cornelius, L. A.; Das, J.; Doweyko, A. M.; Fairchild, C.; Hunt, J. T.; Inigo, I.; Johnston, K.; Kamath, A.; Kan, D.; Klei, H.; Marathe, P.; Pang, S.; Peterson, R.; Pitt, S.; Schieven, G. L.; Schmidt, R. J.; Tokarski, J.; Wen, M. L.; Wityak, J.; Borzilleri, R. M. Discovery of *N*-(2-chloro-6-methyl-phenyl)-2-(6-(4-(2-hydroxyethyl)-piperazin-1-yl)-2-methylpyrimidin-4-yl-amino)thiazole-5-carboxamide (BMS-354825), a dual Src/Abl kinase inhibitor with potent antitumor activity in preclinical assays. *J. Med. Chem.* **2004**, *47* (27), 6658–6661.
- Garnett, M. J.; Marais, R. Guilty as charged: B-RAF is a human oncogene. *Cancer Cell* **2004**, *6* (4), 313–319.
- Niculescu-Duvaz, I.; Roman, E.; Whittaker, S. R.; Friedlos, F.; Kirk, R.; Scanlon, I. J.; Davies, L. C.; Niculescu-Duvaz, D.; Marais, R.; Springer, C. J. Novel inhibitors of B-RAF based on a disubstituted pyrazine scaffold. Generation of a nanomolar lead. *J. Med. Chem.* **2006**, *49* (1), 407–416.
- Niculescu-Duvaz, I.; Roman, E.; Whittaker, S.; Friedlos, F.; Kirk, R.; Scanlon, I.; Davies, L. C.; Niculescu-Duvaz, D.; Marais, R.; Springer, C. J. Novel inhibitors of the v-raf murine sarcoma viral oncogene homologue B1 (BRAF) based on a 2,6-disubstituted pyrazine scaffold. *J. Med. Chem.* **2008**, *51* (11), 3261–3274.
- Niculescu-Duvaz, D.; Gaulon, C.; Dijkstra, H. P.; Niculescu-Duvaz, I.; Zambon, A.; Ménard, D.; Suijkerbuijk, B. M. J. M.; Nourry, A.; Davies, L.; Manne, H.; Friedlos, F.; Ogilvie, L.; Hedley, D.; Whittaker, S.; Kirk, R.; Gill, A.; Taylor, R. D.; Raynaud, F. I.; Moreno-Farre, J.; Marais, R.; Springer, C. J. Pyridoimidazolones as novel potent inhibitors of v-Raf murine sarcoma viral oncogene homologue B1 (BRAF). *J. Med. Chem.* **2009**, *52* (8), 2255–2264.
- Ménard, D.; Niculescu-Duvaz, I.; Dijkstra, H. P.; Niculescu-Duvaz, D.; Suijkerbuijk, B. M. J. M.; Zambon, A.; Nourry, A.; Roman, E.; Davies, L.; Manne, H. A.; Friedlos, F.; Kirk, R.; Whittaker, S.; Gill, A.; Taylor, R. D.; Marais, R.; Springer, C. J. Novel potent BRAF inhibitors: toward 1 nM compounds through optimization of the central phenyl ring. *J. Med. Chem.* **2009**, *52* (13), 3881–3891.
- Nourry, A.; Zambon, A.; Davies, L.; Niculescu-Duvaz, I.; Dijkstra, H. P.; Ménard, D.; Gaulon, C.; Niculescu-Duvaz, D.; Suijkerbuijk, B. M. J. M.; Friedlos, F.; Manne, H. A.; Kirk, R.; Whittaker, S.; Marais, R.; Springer, C. J. BRAF inhibitors based on an imidazo-[4,5]pyridin-2-one scaffold and a meta substituted middle ring. *J. Med. Chem.* DOI: 10.1021/jm901509a.
- Gallou, I.; Eriksson, M.; Zeng, X. Z.; Senanayake, C.; Farina, V. Practical synthesis of unsymmetrical ureas from isopropenyl carbamates. *J. Org. Chem.* **2005**, *70* (17), 6960–6963.
- Regan, J.; Breitfelder, S.; Cirillo, P.; Gilmore, T.; Graham, A. G.; Hickey, E.; Klaus, B.; Madwed, J.; Moriaki, M.; Moss, N.; Pargellis, C.; Pav, S.; Proto, A.; Swinamer, A.; Tong, L.; Torcellini, C. Pyrazole urea-based inhibitors of p38 MAP kinase: from lead compound to clinical candidate. *J. Med. Chem.* **2002**, *45* (14), 2994–3008.
- Whittaker, S.; Marais, R. Unpublished results.
- Ghose, A. K.; Herbertz, T.; Pippin, D. A.; Salvino, J. M.; Mallamo, J. P. Knowledge based prediction of ligand binding modes and

- rational inhibitor design for kinase drug discovery. *J. Med. Chem.* **2008**, *51* (17), 5149–5171.
- (32) Liao, J. J. L. Molecular recognition of protein kinase binding pockets for design of potent and selective kinase inhibitors. *J. Med. Chem.* **2007**, *50* (3), 409–424.
- (33) Liu, Y.; Gray, N. S. Rational design of inhibitors that bind to inactive kinase conformations. *Nat. Chem. Biol.* **2006**, *2* (7), 358–364.
- (34) Jones, G.; Willett, P.; Glen, R. C.; Leach, A. R.; Taylor, R. Development and validation of a genetic algorithm for flexible docking. *J. Mol. Biol.* **1997**, *267* (3), 727–748.
- (35) Smith, N. F.; Hayes, A.; Nutley, B. P.; Raynaud, F. I.; Workman, P. Evaluation of the cassette dosing approach for assessing the pharmacokinetics of geldanamycin analogues in mice. *Cancer Chemother. Pharmacol.* **2004**, *54*, 475–486.
- (36) Nutley, B. P.; Raynaud, F. I.; Wilson, S. C.; Fischer, P.; Hayes, A.; Goddard, P. M.; McClue, S. J.; Jarman, M.; Lane, D. P.; Workman, P. Metabolism and pharmacokinetics of the cyclin-dependent kinase inhibitor *R*-roscovitine in the mouse. *Mol. Cancer Ther.* **2005**, 4125–4139.
- (37) Workman, P.; Twentyman, P.; Balkwill, F.; Balmain, A.; Chaplin, D.; Double, J.; Embleton, J.; Newell, D.; Raymond, R.; Stables, J.; Stephens, T.; Wallace, J. United Kingdom Co-Ordinating Committee on Cancer Research (UKCCCR). Guidelines for the welfare of animals in experimental neoplasia (2nd ed.). *Br. J. Cancer* **1998**, *77* (1), 1–10.